

# Bridging GANs and Bayesian Neural Networks via Partial Stochasticity

Maurizio Filippone<sup>1</sup> Marius P. Linhard<sup>2</sup>

## Abstract

Generative Adversarial Networks (GANs) are popular and successful generative models. Despite their success, optimization is notoriously challenging. In this work, we explain the success and limitations of GANs by casting them as Bayesian neural networks with partial stochasticity. This interpretation allows us to establish conditions of universal approximation and to rewrite the adversarial-style optimization of several variants of GANs as the optimization of a proxy for the likelihood obtained by marginalizing out the stochastic variables. Following this interpretation, the need for regularization becomes apparent, and we propose to adopt strategies to smooth the loss landscape and methods to search for solutions with minimum description length, which are associated with flat minima and good generalization. Results obtained on a wide range of experiments indicate that these strategies lead to performance improvements and pave the way to a deeper understanding of GANs.

## 1. Introduction

Generative Adversarial Networks (GANs) (Goodfellow et al., 2014) are a popular and powerful class of generative models originally conceived for artificial curiosity (Schmidhuber, 1990; 1991). GANs have shown impressive performance, e.g., in generating realistic-looking images in computer vision applications (see, e.g., Karras et al. (2020b); Wang et al. (2023b)). A notoriously difficult aspect of GANs is their optimization, and we speculate that this is the reason why the literature on generative modeling has recently shifted its focus to diffusion models. However, GANs remain attractive because once trained, the cost of generating one sample is as low as one model evaluation, while diffusion models require more computational effort (Zheng et al., 2023).

In this work, our aim is to revive the interest in GANs by

<sup>1</sup>Statistics Program, KAUST, Saudi Arabia <sup>2</sup>RPTU Kaiserslautern-Landau, Germany. Correspondence to: Maurizio Filippone <maurizio.filippone@kaust.edu.sa>.

Preprint. February 3, 2026.

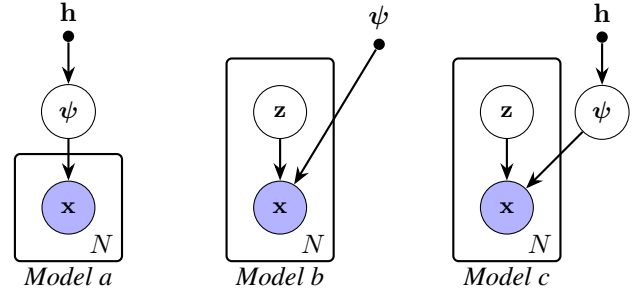


Figure 1. Graphical model representation of various BNNs studied in this work. We use the standard convention that nodes denote stochastic random variables, while dots represent deterministic ones. Shaded nodes denote observed variables, and we use the plate notation to indicate that certain random variables have  $N$  repetitions. *Model a* represents a BNN with full stochasticity for generative modeling (e.g., Tran et al. (2021)). *Model b* represents BNNs with partial stochasticity, where all stochasticity is captured by  $z$  (Sharma et al., 2023); this is the construction that we use to study of GANs in this work. *Model c* is the graphical model of Bayesian GANs (Saatci & Wilson, 2017).

studying them as Bayesian neural networks (BNNs) with partial stochasticity (Sharma et al., 2023), allowing us to advance our understanding of their success and limitations. In our analysis, we introduce a set of random variables  $p(z) = \mathcal{N}(z|\mathbf{0}, \mathbf{I})$  that is transformed into a set of random variables  $x$  through a function  $f_{\text{gen}}(z, \psi)$  parameterized by a neural network (*a.k.a.* the generator) with parameters  $\psi$  (Bishop et al., 1998; MacKay, 1995). This construction is considered partially stochastic because all stochasticity is encapsulated in  $z$ , while neural network parameters are deterministic (*Model b* in Figure 1).

The first insight into the success of GANs comes from the literature on BNNs (Neal, 1996; Mackay, 1994); we can adapt recent results on BNNs with partial stochasticity (Sharma et al., 2023) to establish that GANs are universal approximators of any absolutely continuous distribution over  $x$ , provided that the dimensionality of latent variables is large enough and that the generator satisfies the standard conditions of universal function approximation (Leshno et al., 1993). In other words, partial stochasticity leads to sufficiently expressive BNNs, compared to fully stochastic BNNs where neural network parameters are considered stochastic and they have a prior conditioned on some hyper-parameters

h (Tran et al., 2021) (*Model a* in Figure 1).

The second insight into the success of GANs comes from the analysis of the likelihood of the corresponding graphical model. After defining the latent variables  $\mathbf{Z} = \{z_i\}_{i=1,\dots,N}$  associated with the training data  $\mathbf{X}$ , we would like to integrate these variables out as  $\int p(\mathbf{X}|\mathbf{Z}, \psi)p(\mathbf{Z})d\mathbf{Z}$  to obtain the marginalized likelihood  $p(\mathbf{X}|\psi)$ . However, the intractability of this objective prevents us from being able to optimize it with respect to  $\psi$ .

In this paper, we show that this marginalized likelihood can be rewritten as the Kullback-Leibler (KL) divergence between  $\pi(\mathbf{x})$ , the true generating distribution, and  $p(\mathbf{x}|\psi)$ . We can then derive the objective of many popular GANs by replacing the KL divergence with alternative matching objectives. Interestingly, computing many popular matching objectives requires the definition and optimization of a discriminator, which then becomes an accessory to GANs optimization. Another notable aspect is that the objective is designed so that it can be optimized using samples from  $\pi(\mathbf{x})$ , that is, our training set  $\mathbf{X}$ , and samples from the model  $p(\mathbf{x}|\psi)$ , which are easy to obtain. We can cast several GANs within our unified framework, and we report in particular on standard GANs (Goodfellow et al., 2014), Generative Adversarial Networks with  $f$ -divergences ( $f$ -GANs) (Nowozin et al., 2016), Wasserstein Generative Adversarial Networks (W-GANs) (Arjovsky et al., 2017), and Maximum Mean Discrepancy Generative Adversarial Networks (MMD-GANs) (Dziugaite et al., 2015; Li et al., 2017).

Our analysis of GANs as BNNs with partial stochasticity reveals their limitations too. GANs effectively perform some form of maximum likelihood. Viewed through these lenses, it is clear that there is no intrinsic mechanism to control overfitting, and if the model is too flexible it can assign large values of  $p(\mathbf{X}|\psi)$  on the training data, which is undesirable.

This realization motivates us to propose various ways to improve GANs. One line of investigation is to introduce regularization as a means to improve generalization, and we propose likelihood relaxation and gradient regularization (Arjovsky & Bottou, 2017; Roth et al., 2017; Nagarajan & Kolter, 2017). Another line of attack is to encourage optimization to obtain solutions associated with good generalization. The connection between Occam’s razor, minimum description length (low Kolmogorov complexity), and flat minima (Solomonoff, 1964; Hochreiter & Schmidhuber, 1997; Schmidhuber, 1995), motivates us to study ways to optimize parameters by guiding the optimization toward flat minima (Hochreiter & Schmidhuber, 1997; Foret et al., 2021). A third line of study is to treat model parameters in an approximate Bayesian way to reap their intrinsic benefits of regularization through ensembling (Saatci & Wilson, 2017) (*Model C* in Figure 1). In order to keep a practical implementation of GANs, we will adopt Monte Carlo

Dropout (MCD) (Gal & Ghahramani, 2016), which has been shown to be an instance of variational inference and it is straightforward to adopt.

Through extensive experiments, we support the conclusion that these strategies are effective in improving generative modeling performance in GANs. The main contributions of this paper are as follows:

**Deriving GANs objectives from first principles.** In Section 3, we show that various popular GANs target tractable sample-based proxies for the intractable likelihood obtained by marginalizing out the random variables  $\mathbf{z}$ . More specifically, these proxies can be estimated through samples from the model and data;

**Deriving approximation guarantees for GANs.** In Section 4, we build on recent results on BNNs with partial stochasticity to establish the conditions enabling GANs to be universal approximators of any absolutely continuous distribution over  $\mathbf{x}$ ;

**Understanding and improving GANs.** In Section 6, we leverage our improved understanding of GANs to empirically demonstrate that model regularization, flat minima search, and approximate inference generally enable GANs to achieve higher generation quality compared to standard optimization.

## 2. Background

We consider a generative modeling task for a random variable  $\mathbf{x}$  taking values in  $\mathcal{X} \subseteq \mathbb{R}^D$ , starting from a dataset  $\mathbf{X} = \{\mathbf{x}_1, \dots, \mathbf{x}_N\}$ , where the samples  $\mathbf{x}_i$  are drawn i.i.d. from an unknown distribution with associated density  $\pi(\mathbf{x})$ . Throughout this paper, we consider random variables whose probability measure is absolutely continuous with respect to the  $D$ -dimensional Lebesgue measure. To simplify the exposition, we use  $\pi(\mathbf{x})$  to denote both the probability distribution and its density function. Similarly, we use  $\mathbf{x}$  to represent both the random variable and its realization.

### Probabilistic Generative Models using Neural Networks

We can set up a probabilistic model for this task as follows. Let’s introduce a set of latent variables  $\mathbf{Z} = \{z_1, \dots, z_N\}$ , with  $z_i \in \mathbb{R}^P$  and a parametric model  $p(\mathbf{x}|\mathbf{z}, \psi)$ . The parameters  $\psi$  refer to the ones of a neural network  $\mathbf{f}_{\text{gen}}(z_i, \psi)$  mapping latent variables  $z_i$  into corresponding  $\mathbf{x}_i$ . In a parallel with GANs, we consider a deterministic generator, so the likelihood can be written as:

$$p(\mathbf{x}_i|z_i, \psi) = \delta(\mathbf{x}_i - \mathbf{f}_{\text{gen}}(z_i, \psi)), \quad (1)$$

where  $\delta$  is Dirac’s delta. This construction takes the input distribution over latent variables  $\mathbf{z}$  and turns it into a flexible distribution over  $\mathbf{x}$ . This class of latent variable models is known under several names in the literature (MacKay,

1995; Bishop et al., 1998; Nowozin et al., 2016), and we will refer to these as generative neural samplers, or, more simply, as generators. In this work, we interpret these latent variable models as BNNs with partial stochasticity (*Model b* in Figure 1). In this interpretation, the random variables  $\mathbf{z}$  in input are transformed into  $\mathbf{x}$  through a mapping  $\mathbf{f}_{\text{gen}}(\mathbf{z}_i, \psi)$ ; parameters are considered deterministic (to be optimized) and all the stochasticity of this model is captured by  $\mathbf{z}$ .

Following common practice in latent variables models, we can attempt to integrate out the latent variables  $\mathbf{Z}$

$$p(\mathbf{X}|\psi) = \int p(\mathbf{X}|\mathbf{Z}, \psi)p(\mathbf{Z}) d\mathbf{Z}, \quad (2)$$

with the aim of maximizing this objective with respect to  $\psi$ . A closer inspection of the integral above, under the factorization of the likelihood  $p(\mathbf{X}|\mathbf{Z}, \psi) = \prod_i p(\mathbf{x}_i|\mathbf{z}_i, \psi)$  indicates that we can gracefully factorize the marginalized likelihood  $p(\mathbf{X}|\psi)$  as the product of individual data-specific marginalized likelihood terms:

$$p(\mathbf{X}|\psi) = \prod_i \int p(\mathbf{x}_i|\mathbf{z}_i, \psi)p(\mathbf{z}_i) d\mathbf{z}_i = \prod_i p(\mathbf{x}_i|\psi).$$

Optimizing (the logarithm of) this objective directly is challenging because it is intractable to marginalize out latent variables in interesting scenarios where  $D$  and  $P$  are even moderately large and  $\mathbf{f}_{\text{gen}}(\mathbf{z}_i, \psi)$  is implemented by a neural network. Up to a scaling factor of  $1/N$ , we can interpret this objective as a Monte Carlo average of the following expectation (*a.k.a.* expected risk):

$$\psi_* = \arg \max_{\psi} \mathbb{E}_{\pi(\mathbf{x})} \{ \log [p(\mathbf{x}|\psi)] \}, \quad (3)$$

which we will use as a starting point of our analysis in the next section.

### 3. A Practical Proxy for the Likelihood

For reasons that will be apparent soon, let  $P \geq D$ . Simple manipulations of Equation (3) show that the optimization of the marginalized likelihood can be rewritten equivalently as (Akaike, 1973; Tran et al., 2021):

$$\psi_* = \arg \min_{\psi} \text{KL} [\pi(\mathbf{x}) \| p(\mathbf{x}|\psi)]. \quad (4)$$

The assumption that  $P \geq D$  ensures that the divergence is not degenerate. This result says that the optimal model is the one which minimizes the KL divergence between the true generating distribution and the one characterized by our generative model. However, this reformulation does not immediately simplify the optimization problem. This is because we can only access samples from  $\pi(\mathbf{x})$ , and there is no closed form for the density  $p(\mathbf{x}|\psi)$ ; while it

is straightforward to obtain samples from  $p(\mathbf{x}|\psi)$ , sample-based estimators of the KL divergence through samples typically have large variance (Flam-Shepherd et al., 2017; Tran et al., 2022).

For completeness, here is how to obtain samples from the two distributions of interest. For  $\pi(\mathbf{x})$ , we have samples  $\mathbf{x}_i$ , that is our data. For  $p(\mathbf{x}|\psi)$ , we can sample  $\mathbf{z}$  from  $\mathcal{N}(\mathbf{z}|\mathbf{0}, \mathbf{I})$  and then  $\mathbf{x}$  from  $p(\mathbf{x}|\mathbf{z}, \psi)$ ; this yields samples from the joint  $p(\mathbf{x}, \mathbf{z}|\psi)$ , which is what we need to obtain samples from  $p(\mathbf{x}|\psi)$  if we disregard  $\mathbf{z}$ .

#### 3.1. Replacing the KL divergence with other divergences or integral probability metrics.

We can exploit the equivalence between marginal likelihood optimization and the matching of  $\pi(\mathbf{x})$  and  $p(\mathbf{x}|\psi)$  to derive tractable objectives, which turn out to be the objectives of popular GANs. In particular, we can replace the KL divergence with alternatives aimed at achieving the same objective of matching  $p(\mathbf{x}|\psi)$  to the true generating distribution  $\pi(\mathbf{x})$ . Here we have a number of choices, and we can draw from the literature on other divergences (e.g.,  $f$ -divergences (Nguyen et al., 2007; Gneiting & Raftery, 2007)) or integral probability metrics (Müller, 1997) (e.g., 1-Wasserstein distance (Villani, 2016) or Maximum Mean Discrepancy (MMD) (Gretton et al., 2006)). The result is a series of GAN formulations, which we discuss shortly.

Note that, Equation (4) establishes an alternative formulation for the optimization of the marginalized likelihood as the optimization of a KL divergence. It would be interesting to use this equivalence in the opposite direction and derive the “generalized marginalized likelihoods” stemming from the use of other divergences or integral probability metrics. We find this challenging due to the form of the matching objectives that in general entangle  $p(\mathbf{x}|\psi)$  and  $\pi(\mathbf{x})$  in a way that prevents expressing the left hand side as an expectation over  $\pi(\mathbf{x})$  of a function of  $p(\mathbf{x}|\psi)$ , which is needed to interpret this as an expected risk. While this might be possible for some particular matching objectives, we leave this investigation for future works.

Note also that the discriminator, which does not appear in the formulation of latent variable models or BNNs with partial stochasticity, becomes an essential component of GANs, as it is generally needed to calculate matching objectives.

**GANs.** Up to some constants, the objective of the original GANs in Goodfellow et al. (2014) is:

$$\psi_* = \arg \min_{\psi} \text{JS}[\pi(\mathbf{x})||p(\mathbf{x}|\psi)], \quad (5)$$

where JS is the Jensen-Shannon divergence:

$$\text{JS}[p(\mathbf{x})||q(\mathbf{x})] = \frac{1}{2} \text{KL} [p(\mathbf{x}) \| a(\mathbf{x})] + \frac{1}{2} \text{KL} [q(\mathbf{x}) \| a(\mathbf{x})],$$

with  $a(\mathbf{x}) = \frac{1}{2}(p(\mathbf{x}) + q(\mathbf{x}))$ .

***f*-GANs.** Nowozin et al. (2016) present a more general class of GANs with objectives derived from *f*-divergences

$$\mathcal{D}_f(\pi(\mathbf{x})\|p(\mathbf{x}|\psi)) = \int p(\mathbf{x}|\psi) f\left(\frac{\pi(\mathbf{x})}{p(\mathbf{x}|\psi)}\right) d\mathbf{x},$$

for which the Jensen-Shannon divergence is a special case. Their work leverages variational methods to tractably estimate *f*-divergences between distributions through samples (Nguyen et al., 2007).

**W-GANs.** Within the family of integral probability metrics, we find the popular 1-Wasserstein distance. If we replace the KL divergence in Equation (4) with this metric, we can cast optimization as:

$$\arg \min_{\psi} \{W_1(\pi(\mathbf{x}), p(\mathbf{x}|\psi))\}.$$

We can use a dual formulation of the 1-Wasserstein distance to obtain the following objective:

$$\arg \min_{\psi} \left\{ \sup_{\text{Lip}(f) \leq 1} (\mathbb{E}_{\pi(\mathbf{x})}[f(\mathbf{x})] - \mathbb{E}_{p(\mathbf{x}|\psi)}[f(\mathbf{x})]) \right\}.$$

This approach is essentially the one presented in the W-GAN paper (Arjovsky et al., 2017). The discriminator is modeled as a neural network, and the Lipschitz condition can be imposed either by adding a regularization term to the discriminator (Gulrajani et al., 2017) or by construction (Ducotterd et al., 2024).

**MMD-GAN.** MMD (Gretton et al., 2006) is another member of the family of integral probability measures. Replacing the KL divergence in Equation (4) with the MMD, we obtain a similar objective to the W-GAN, except that the discriminator is now a function in a Reproducing Kernel Hilbert Space (RKHS) denoted by  $\mathcal{H}$ :

$$\arg \min_{\psi} \left\{ \sup_{f \in \mathcal{H}, \|f\|_{\mathcal{H}} \leq 1} (\mathbb{E}_{\pi(\mathbf{x})}[f(\mathbf{x})] - \mathbb{E}_{p(\mathbf{x}|\psi)}[f(\mathbf{x})]) \right\}.$$

In practice, it is convenient to square the MMD distance so that the objective has a closed form, and it can be expressed through the evaluation of the kernel function  $k(\cdot, \cdot)$  with samples from the two distributions as input. The objective lends itself to an unbiased estimate over mini-batches (Gretton et al., 2012). The use of MMD as a matching objective was proposed in Dziugaite et al. (2015), who also provide generalization bounds of the resulting MMD-GAN. For discussions on the choice/optimization of a kernel function and  $\sqrt{\mathcal{L}_{\text{MMD}^2}}$  as a loss, we refer the reader to Li et al. (2015; 2017); Dziugaite et al. (2015).

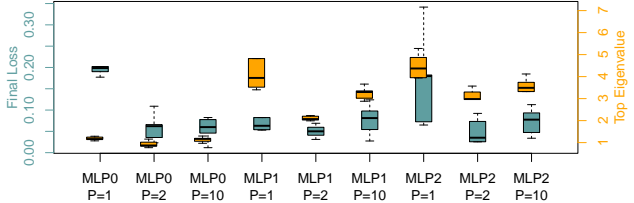


Figure 2. MMD-GANs on two-dimensional Gaussian data. Details on the experimental setup in the main text.

### 3.2. Understanding Overfitting in GANs

We illustrate the issue of overfitting in GANs on a simple generative modeling problem, where the dataset contains  $N = 2000$  input vectors drawn from a zero-mean and unit-variance Gaussian distribution with  $D = 2$ . We consider three possible latent dimensions  $P = 1, 2, 10$  and three possible architectures for the generator: MLP0 indicates a Multi Layer Perceptron (MLP) with zero hidden layers (linear model), and MLP1 and MLP2 indicate MLPs with one and two hidden layers, respectively. The number of hidden units is set to 64. We train MMD-GANs (Dziugaite et al., 2015) with all possible combinations of latent dimensions and generator architectures. For the discriminator, we adopt an MLP with two hidden layers with 64 hidden units. Each run is repeated five times.

In Figure 2, we report a boxplot of the value of the objective obtained at the end of the optimization and a boxplot of the top eigenvalue of the Hessian of the objective. When the latent dimensionality is too low ( $P < D$ ), the model is unable to attain good solutions, as indicated by the high value of the objective at the end of optimization, regardless of how complex the generator is. When  $P > D$ , all configurations reach a good solution, indicating a close match between the generated and true distributions. However, complex models are characterized by sharp minima (large top eigenvalue). The model with the right level of complexity (MLP0 with  $P = 2$ ) shows that the solution obtained is indeed characterized by a flat loss landscape at the optimum.

### 3.3. Regularization to Smooth Out the Loss Landscape

**Likelihood relaxation** One of the most striking features emerging from viewing GANs as latent variable models is that the likelihood is a degenerate Dirac’s delta, with no aleatoric uncertainty. Such a degeneracy of the likelihood is due to the constraint that one latent variable  $\mathbf{z}$  has to be associated with one  $\mathbf{x}$ . A sensible relaxation is to turn the Dirac’s delta into a Gaussian likelihood  $\mathcal{N}(\mathbf{x}_i | \mathbf{f}_{\text{gen}}(\mathbf{z}_i, \psi), \sigma_{\text{lik}}^2)$ , meaning that the generator produces  $\mathbf{x} = \mathbf{f}_{\text{gen}}(\mathbf{z}_i, \psi) + \epsilon$  with  $\epsilon \sim \mathcal{N}(\epsilon | 0, \sigma_{\text{lik}}^2)$  during training. Previous works have considered this form on noise perturbation to improve the stability of GANs optimization (Arjovsky & Bottou, 2017;

Roth et al., 2017). From a statistical perspective, we can understand this simple change as a likelihood relaxation aimed at improving model robustness, and we will demonstrate the effectiveness of this strategy in the experiments. When generating images to evaluate performance, we just compute  $\mathbf{f}_{\text{gen}}(\mathbf{z}_i, \psi)$  without adding noise.

**Gradient Regularization** Another technique to smooth the loss landscape in GANs is gradient regularization, which has been discussed, e.g., in Nagarajan & Kolter (2017):

$$\hat{\psi} = \arg \max_{\psi} \left\{ \log [p(\mathbf{X}|\psi)] - \lambda_{\text{gr}} \|\nabla_{\psi} \log [p(\mathbf{X}|\psi)]\|^2 \right\}.$$

For any GANs, the logarithm of the marginalized likelihood  $\log [p(\mathbf{X}|\psi)]$  is then replaced by the corresponding generator loss. The regularization pertains to the generator, so only its optimization is affected by this change.

### 3.4. Searching for Flat Minima

**Small batch sizes.** One way to avoid sharp minima is to operate with noisy stochastic gradients, which can be achieved with small batch sizes. This strategy is a well-known implicit form of regularization (see, e.g., Brock et al. (2019); Fatras et al. (2020)). While a larger variance of the stochastic gradients adds to the instability of the optimization, various implementations of GANs available in the literature have indeed settled for a small batch size and a corresponding small learning rate, and we speculate that this is to reap the effects of the induced regularization while keeping the optimization stable to some extent.

**Sharpness-Aware Minimization.** Sharpness-Aware Minimization (SAM) is a popular technique for searching for flat minima in the parameter space (Foret et al., 2021; Hochreiter & Schmidhuber, 1997). SAM operates by performing a standard stochastic gradient step, followed by a maximization of the objective in the neighborhood of radius  $\rho_{\text{SAM}}$ . The rationale is that, in flat minima, the second step does not deteriorate the objective much, and the optimizer is encouraged to look for such solutions. We are not aware of previous attempts to use SAM in GANs.

### 3.5. Approximate Inference

Another strategy to improve GANs is to carry out approximate inference of model parameters (*Model c* in Figure 1). This was previously considered in Saatci & Wilson (2017), where they adopt Markov chain Monte Carlo inference of the parameters of the generator and the discriminator. Given the huge computational cost associated with this approach, we consider MCD as an alternative to carry out approximate (variational) inference of model parameters (Gal & Ghahramani, 2016). This can be easily implemented by introducing dropout layers in the generator and discriminator.

## 4. Partially Stochastic Networks.

We now establish approximation guarantees for GANs by casting them as BNNs with partial stochasticity. By adapting the theoretical framework in Sharma et al. (2023), we derive universal approximation properties for any absolutely continuous distribution  $\pi(\mathbf{x})$ . To achieve this, we first define the requirements for the generator’s architecture.

**Assumption 4.1.** The generator architecture  $\mathbf{f}_{\text{gen}}(\cdot, \psi) : \mathbb{R}^P \rightarrow \mathcal{X}$  satisfies the conditions in Leshno et al. (1993), ensuring it can approximate any continuous function  $\tilde{\mathbf{f}}(\cdot) : \mathbb{R}^P \rightarrow \mathcal{X}$  with arbitrary precision

Under this assumption, we present the main theorem establishing that GANs, viewed as BNNs with partial stochasticity, are universal approximators of probability distributions.

**Theorem 4.2.** (Adapted from Sharma et al. (2023)). *Let  $\mathbf{x}$  be a random variable in  $\mathcal{X} \subseteq \mathbb{R}^D$  and  $\mathbf{f}_{\text{gen}}(\cdot, \psi) : \mathbb{R}^P \rightarrow \mathcal{X}$  be a neural network satisfying Theorem 4.1. Let  $\mathbf{z}$  be Gaussian-distributed random variables with finite mean and variance. If there exists a continuous generator function  $\tilde{\mathbf{f}}(\cdot) : \mathbb{R}^P \rightarrow \mathcal{X}$  that induces the distribution of  $\mathbf{x}$  from the latent noise, then  $\mathbf{f}_{\text{gen}}(\cdot, \psi)$  can approximate it arbitrarily well. Specifically,  $\forall \varepsilon > 0, \lambda < \infty$ , there exist parameters  $\psi \in \Psi$ , a scaling matrix  $V \in \mathbb{R}^{P \times P}$  and a shift-vector  $\mathbf{u} \in \mathbb{R}^P$ , such that*

$$\sup_{\eta \in \mathbb{R}^P, |\eta| \leq \lambda} |\mathbf{f}_{\text{gen}}(V\eta + \mathbf{u}, \psi) - \tilde{\mathbf{f}}(\eta)| < \varepsilon.$$

The proof, detailed in Sharma et al. (2023), leverages the noise outsourcing lemma (Austin, 2015) to guarantee the existence of  $\tilde{\mathbf{f}}(\cdot)$ , and the universal approximation theorem (Leshno et al., 1993) to guarantee that the network can represent it.

Informally, these conditions require enough stochasticity in  $\mathbf{z}$  (e.g.,  $P$  large enough) so that the distribution produced by the generator can be mapped to the support of  $\mathbf{x}$ ; in addition, the generator needs to have enough flexibility to be able to transform the distribution over  $\mathbf{z}$  into any absolutely continuous distribution with density on the support of  $\mathbf{x}$ , and this is ensured by the classic universal approximation theorem for neural networks. In practice, the manifold hypothesis (Loaiza-Ganem et al., 2022; Brown et al., 2023) suggests that most large-dimensional datasets live in a low-dimensional manifold, which then relaxes the need to set  $P \geq D$ , and indeed in practice GANs work extremely well with  $P \ll D$  for such applications.

### 4.1. Graphical Models and Model Selection

The theory helps us to establish conditions for ensuring universal approximation; however, the theory does not give practical advice on how to precisely determine the architecture and how to introduce the necessary stochasticity. In

Figure 1, under the right conditions, the three BNN models have the same expressivity in approximating  $\pi(\mathbf{x})$ . *Model a* is the Bayesian AutoEncoder in Tran et al. (2021), where the generator is simply an AutoEncoder whose parameters are inferred (through Markov chain Monte Carlo sampling) rather than optimized. In this case, full stochasticity is encoded in the parameters, while in GANs, partial stochasticity is encapsulated in  $\mathbf{z}$  (*Model b* in Figure 1). *Model c* in Figure 1 is the Bayesian GAN in Saatci & Wilson (2017). Again, the theory of BNNs with partial stochasticity does not favor one approach over the others, as long as the corresponding architectures satisfy Theorem 4.1 and  $P$  is large enough, so model selection should ultimately be used to determine these choices.

## 5. Related Works

**Improving the training dynamics of GANs.** Training GANs is notoriously challenging, and divergent optimization dynamics is a common problem. GANs are supposed to converge to a Nash equilibrium, but this may not always exist (Farnia & Ozdaglar, 2020). In order to alleviate this problem, there are various lines of work. Farnia & Ozdaglar (2020) propose to relax the constraint of Nash equilibrium and introduce a new training algorithm accordingly. Focusing on optimization but without relaxing the Nash equilibrium, Nie & Patel (2020) propose a way to regularize the Jacobian of the training dynamics. Sinha et al. (2020) propose the Top-k Training, where only the best generated samples are used to perform updates and train the generator. Huang et al. (2024), on the other hand, combine both architectural changes and gradient regularization of the discriminator to improve the training dynamics of Relativistic Generative Adversarial Networks (R-GANs) (Jolicœur-Martineau, 2019). Adapting the architecture in the STYLE-GAN2 paper (Karras et al., 2020b) they introduce a new baseline for GANs, which they name R3-GAN. After proving that this indeed leads to local convergence, Huang et al. (2024) empirically show that this new baseline is able to achieve state-of-the-art performance.

**GANs as probabilistic generative models.** We view GANs as probabilistic generative models, where a set of latent variables is mapped to the input space through a neural network (MacKay, 1995; Bishop et al., 1998). In this interpretation, these are instances of BNNs (Neal, 1996; Mackay, 1994) with partial stochasticity (Sharma et al., 2023). Unlike previous work on generative models with full network stochasticity (Saatci & Wilson, 2017; Tran et al., 2021), in the probabilistic view of GANs, network parameters are treated deterministically and epistemic uncertainty is captured by the distribution over latent variables. Tran et al. (2021) consider generative models in the form of auto-encoders, and more works exploring the connections between GANs and auto-encoders (Variational Autoencoder (VAE) in particular)

include Mescheder et al. (2017); Balaji et al. (2019). It is worth mentioning previous work by Tiao et al. (2018), who carry out a variational analysis of latent variable models with an implicitly-defined prior over latent variables, which leads to a family of models that includes CYCLE-GANs (Zhu et al., 2017) as a special case.

**Regularizing the generator.** Regularization is a successful strategy to improve GANs optimization. In the literature, however, a lot of effort has been dedicated to the improvement of statistical properties of the discriminator to improve optimization stability (Gulrajani et al., 2017; Wu et al., 2018). Our work suggests that regularization plays an important role in improving the statistical properties of the generator. For instance, gradient norm regularization of the generator has been studied in Nagarajan & Kolter (2017), while adding noise to the generated samples has been considered in Arjovsky et al. (2017); Roth et al. (2017).

**Latest architectures and objectives.** Karras et al. (2018) propose the STYLE-GAN architecture, which forms the basis of state-of-the-art GAN models. They consider the R-GAN objective and propose a novel mechanism to handle the latent variables by introducing them within the layers of the generator. STYLE-GAN2 (Karras et al., 2020b) was later proposed as an improvement over STYLE-GAN, by tackling the problem of artifacts in the generated images through regularization and architectural improvements. STYLE-GAN2 was then further improved in Karras et al. (2020a) through an adaptive discriminator augmentation (STYLE-GAN2-ADA), and in Karras et al. (2021) using Fourier features, which improves generating quality for videos.

## 6. Experiments

### 6.1. Deep Convolutional GANs

In this section, we validate the hypothesis that introducing regularization or searching for flat minima improves generative modeling performance. We consider experiments on standard benchmark data, including MNIST, CIFAR-10, FFHQ<sup>1</sup>, and CELEBA<sup>2</sup>. All models are optimized for 250 epochs, except for CELEBA for which we train models for 150 epochs. We rescaled the images in MNIST and CIFAR-10 to  $64 \times 64$ , and the ones in FFHQ and CELEBA to  $128 \times 128$ . Scores are computed over 10000 generated images and averaged over three repetitions using the `torch-fidelity` module<sup>3</sup> against .png images resized as above. The results are reported by applying Exponential Moving Average (EMA), with 20 epochs of warm-up and 0.999 decay, reporting standard metrics, such as ISC,

<sup>1</sup><https://github.com/NVLabs/ffhq-dataset.git>

<sup>2</sup><https://mmlab.ie.cuhk.edu.hk/projects/CelebA.html>

<sup>3</sup><https://github.com/toshas/torch-fidelity>

Table 1. Deep Convolutional Generative Adversarial Network (DC-GAN) architecture with Wasserstein divergence objective (Wu et al., 2018) on MNIST, CIFAR-10, FFHQ-128, and CELEBA. Standard deviations, calculated over five seeds times three repetitions of sampling 10 000 images, are reported in parenthesis. The arrows indicate whether metrics are so that the higher the better ( $\uparrow$ ) or the lower the better ( $\downarrow$ ).  $|B|$  denotes the batch size.

W-GAN $ B  = 128$						
STRATEGY	MNIST			CIFAR-10		
	ISC $\uparrow$	FID $\downarrow$	KID $\times 10^{-3}$ $\downarrow$	ISC $\uparrow$	FID $\downarrow$	KID $\times 10^{-3}$ $\downarrow$
NONE $\blacktriangle$	2.27 (0.02)	8.4 (0.4)	6.0 (0.4)	4.64 (0.13)	40.1 (1.5)	30.3 (1.6)
LIKELIHOOD RELAX. ( $\sigma_{\text{lik}}^2 = 0.01$ )	2.27 (0.02)	8.0 (0.4)	5.5 (0.4)	4.74 (0.08)	34.1 (2.2)	24.1 (2.1)
GRADIENT REG. ( $\lambda_{\text{gr}} = 0.01$ )	2.26 (0.01)	8.2 (0.4)	5.8 (0.4)	4.72 (0.08)	37.8 (1.3)	27.9 (1.6)
SAM ( $\rho_{\text{SAM}} = 0.1$ )	2.25 (0.02)	8.6 (0.4)	6.2 (0.5)	4.68 (0.15)	40.6 (3.4)	31.2 (3.5)
MCD ( $p = 0.1$ ) $\triangle$	2.25 (0.02)	7.7 (0.5)	5.4 (0.5)	4.75 (0.05)	38.6 (2.2)	28.7 (2.2)
STRATEGY	FFHQ-128			CELEBA		
	ISC $\uparrow$	FID $\downarrow$	KID $\times 10^{-3}$ $\downarrow$	ISC $\uparrow$	FID $\downarrow$	KID $\times 10^{-3}$ $\downarrow$
NONE $\blacktriangle$	3.21 (0.05)	63.6 (1.5)	55.8 (1.5)	2.87 (0.04)	18.3 (0.9)	12.4 (1.1)
LIKELIHOOD RELAX. ( $\sigma_{\text{lik}}^2 = 0.01$ ) $\triangle$	3.25 (0.04)	62.8 (1.5)	54.8 (1.6)	2.89 (0.05)	17.8 (2.6)	11.5 (2.7)
GRADIENT REG. ( $\lambda_{\text{gr}} = 0.01$ )	3.22 (0.04)	65.1 (3.5)	57.0 (3.4)	2.88 (0.03)	18.5 (0.9)	12.6 (1.1)
SAM ( $\rho_{\text{SAM}} = 0.1$ )	3.26 (0.05)	62.1 (2.0)	53.9 (2.3)	2.84 (0.09)	34.9 (20.8)	28.5 (20.1)
MCD ( $p = 0.05$ )	3.20 (0.06)	65.5 (3.6)	57.4 (3.6)	2.95 (0.13)	42.9 (19.4)	34.9 (18.2)

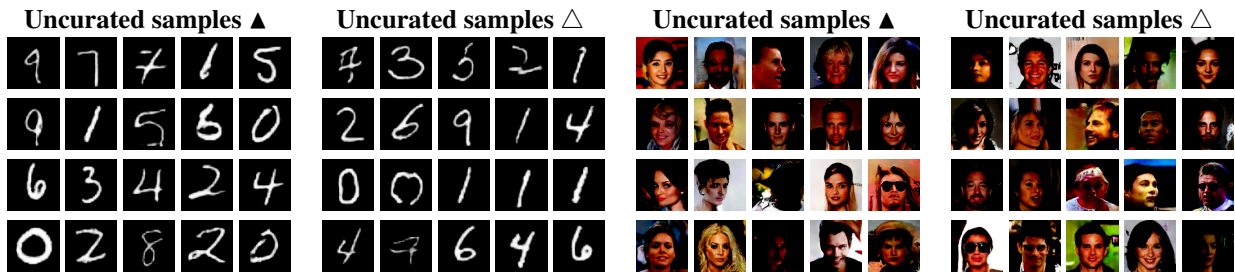


Figure 3. MNIST and CELEBA-uncurated samples generated from the models in Table 1.

FID, and KID. In the Appendix, we also include the top eigenvalue of the Hessian of the objective, estimated using the module `pytorch-hessian-eigenthings`<sup>4</sup>. All experiments are repeated over five different seeds, and we report mean and standard deviation in the tables.

Throughout the experiments, we fix the architecture to be the one proposed in the DC-GAN paper (Radford et al., 2016). We report results on this architecture with the W-GAN objective with divergence regularization (Wu et al., 2018) in Table 1, while in the Appendix we report results for R-GANs, which use the so-called relativistic objective (Jolicoeur-Martineau, 2019). For completeness, in the Appendix we also provide a more comprehensive view of the results obtained by W-GANs on a much broader set of parameters.

We fix the dimensionality of the latent space to  $P = 100$ . For W-GANs, we set the base learning rate to 0.001 for a batch-size  $|B|$  of 128; the learning rate schedule is such

that it reaches the base learning rate after 10 epochs. For R-GANs, we follow the recommendations in previous implementations and set the learning rate to 0.0002. In the experiments where  $\rho_{\text{SAM}} > 0$ , we use (adaptive) SAM for both the generator and the discriminator. In W-GANs, we perform one optimization step for the generator every 5 optimization steps for the discriminator, while for R-GANs we do this after every optimization step of the discriminator. MCD uses one Monte Carlo sample per training iteration and a dropout probability  $p_{\text{MCD}} = 0.1$  for MNIST and CIFAR-10 with dropout layers introduced after the second and third convolutional layers, while  $p_{\text{MCD}} = 0.05$  for FFHQ-128 and CELEBA with dropout layers introduced after the second, third, and fourth convolutional layers. In the Appendix we report results with five Monte Carlo samples per training iteration. Figure 3 show samples associated with some of the configurations reported in Table 1.

For MNIST and CIFAR-10, Table 1 and Table 4 show that, unlike flat minima search, regularization offers consistent improvements. For FFHQ-128 and CELEBA (Table 1 and

<sup>4</sup><https://github.com/noahgolmant/pytorch-hessian-eigenthings>

Table 5), likelihood relaxation improves performance; gradient regularization seems to be effective for a smaller value of the regularization parameter ( $\lambda_{gr} = 0.001$ ).

The results using SAM optimization in Table 1 do not show consistent improvement, indicating that there might be cases for which the simplicity associated with these solutions leads to suboptimal performance for GANs. However, the full set of results in Table 4 and Table 5 also indicate that considerable improvements can be obtained by suitable regularization in combination with SAM. This is particularly the case for CIFAR-10 and CELEBA.

On MNIST and CIFAR-10, MCD obtains a striking consistent improvement in performance. For FFHQ-128 these improvements are less pronounced, while for CELEBA MCD negatively affects performance.

### 6.2. STYLE-GAN2-ADA

In this section, we report experiments on STYLE-GAN2-ADA on the FFHQ dataset rescaled to  $256 \times 256$  (FFHQ256). For this experiment, the baseline is STYLE-GAN2-ADA with the same configuration as Karras et al. (2020a). We test the effect of likelihood relaxation by adding Gaussian noise  $\mathcal{N}(0, \sigma_{lik}^2)$  with  $\sigma_{lik}^2 = 0.001$  to the generated images during training. We train both models until the discriminator has seen 25 million images, and the final FID is 4.30 for the baseline model ( $\blacktriangle$ ) and 4.22 for the one with likelihood relaxation ( $\triangle$ ); samples from the two models can be found in Figure 4. It is interesting to see how adding noise to the generating process indeed leads to performance improvements. This can also be observed after the models see another 5 million images; plain STYLE-GAN2-ADA manages to reduce the FID to 4.11 while our model reaches an FID of 4.07. This experiment suggests that a simple modification to existing implementations of GANs can lead to performance improvements.

## 7. Conclusions

In this paper, we proposed a probabilistic framework based on BNNs with partial stochasticity to understand and improve GANs. This allowed us to establish universal approximation properties of GANs, and to derive the objective of a variety of popular GANs, where the intractable marginalized likelihood objective is replaced by a tractable proxy. This connection gives insights into overfitting, which manifests itself due to the lack of intrinsic regularization. By relying on the connections between Occam’s razor, flat minima, and minimum description length, we studied regularization and optimization strategies to smooth the loss landscape of GANs and to search for flat minima. Overall, while there is no consistent pattern of which configuration is generally superior, the results indicate that the best performance is

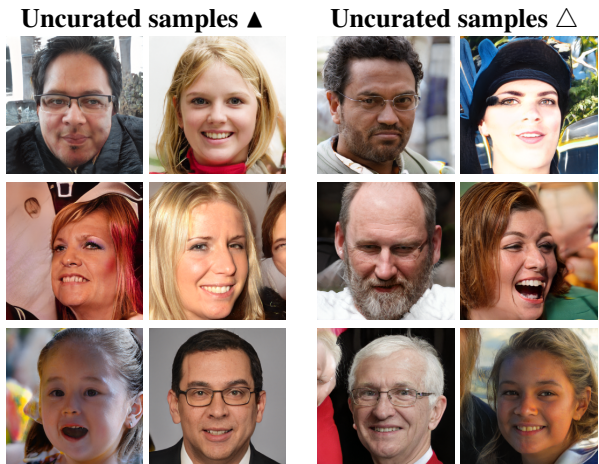


Figure 4. Uncurated samples from the baseline and the one with likelihood relaxation on the FFHQ256 data.

systematically achieved by configurations associated with model regularization, possibly in combination with SAM, and that in certain cases the performance improvement is rather substantial. We hope that this will serve as a starting point for studying strategies to improve the statistical properties of GANs to obtain novel ways to boost their performance and ease optimization. In this work, we kept the GAN architecture fixed, we are interested in studying architecture search in the future. For this, it would be interesting to explore approaches such as Differentiable Architecture Search (DARTS) (Liu et al., 2019), possibly in combination with recent works introducing sparsity in GANs (Wang et al., 2023a).

**Limitations.** Despite the encouraging results, it would be great to find ways to systematically obtain stable optimization and improved performance. For this, it would have been interesting to explore more GAN architectures, objectives, and hyper-parameters to derive general practical guidelines on how to guide these choices. Also, we were hoping to obtain stronger indications on the link between flat minima and good performance; despite this, performance is generally in favor of configurations associated with regularization, possibly combined with SAM optimization.

### Impact Statement

This paper aims to advance the theoretical understanding and practice of GANs. Like other works in the literature of generative modeling, the proposed advancements can have both positive (e.g., synthesizing new data automatically, accelerating drug discovery) and negative (e.g., deep fakes) impacts on society depending on the application.

## Acknowledgements

MF is grateful to Jürgen Schmidhuber for his wonderful seminar series at KAUST and for inspiring several ideas in this paper.

## References

- Akaike, H. Information Theory and an Extension of the Maximum Likelihood Principle. In *2nd International Symposium on Information Theory, 1973*, pp. 268–281. Publishing House of the Hungarian Academy of Sciences, 1973.
- Arjovsky, M. and Bottou, L. Towards Principled Methods for Training Generative Adversarial Networks. In *International Conference on Learning Representations*, 2017.
- Arjovsky, M., Chintala, S., and Bottou, L. Wasserstein Generative Adversarial Networks. In Precup, D. and Teh, Y. W. (eds.), *Proceedings of the 34th International Conference on Machine Learning*, volume 70 of *Proceedings of Machine Learning Research*, pp. 214–223. PMLR, 06–11 Aug 2017.
- Austin, T. Exchangeable random measures. *Annales de l’I.H.P. Probabilités et statistiques*, 51(3):842–861, 2015. doi: 10.1214/13-AIHP584.
- Balaji, Y., Hassani, H., Chellappa, R., and Feizi, S. Entropic GANs meet VAEs: A Statistical Approach to Compute Sample Likelihoods in GANs. In Chaudhuri, K. and Salakhutdinov, R. (eds.), *Proceedings of the 36th International Conference on Machine Learning*, volume 97 of *Proceedings of Machine Learning Research*, pp. 414–423. PMLR, 09–15 Jun 2019.
- Bishop, C. M., Svensén, M., and Williams, C. K. I. GTM: The Generative Topographic Mapping. *Neural Computation*, 10(1):215–234, 1998. doi: 10.1162/089976698300017953.
- Brock, A., Donahue, J., and Simonyan, K. Large Scale GAN Training for High Fidelity Natural Image Synthesis. In *International Conference on Learning Representations*, 2019.
- Brown, B. C., Caterini, A. L., Ross, B. L., Cresswell, J. C., and Loaiza-Ganem, G. Verifying the Union of Manifolds Hypothesis for Image Data. In *International Conference on Learning Representations*, 2023.
- Ducotterd, S., Goujon, A., Bohra, P., Perdios, D., Neumayer, S., and Unser, M. Improving Lipschitz-constrained neural networks by learning activation functions. *J. Mach. Learn. Res.*, 25(1), January 2024. ISSN 1532-4435.
- Dziugaite, G. K., Roy, D. M., and Ghahramani, Z. Training generative neural networks via Maximum Mean Discrepancy optimization. In *Proceedings of the Thirty-First Conference on Uncertainty in Artificial Intelligence, UAI’15*, pp. 258–267, Arlington, Virginia, USA, 2015. AUAI Press. ISBN 9780996643108.
- Farnia, F. and Ozdaglar, A. Do GANs always have Nash equilibria? In III, H. D. and Singh, A. (eds.), *Proceedings of the 37th International Conference on Machine Learning*, volume 119 of *Proceedings of Machine Learning Research*, pp. 3029–3039. PMLR, 13–18 Jul 2020.
- Fatras, K., Zine, Y., Flamary, R., Gribonval, R., and Courty, N. Learning with minibatch Wasserstein : asymptotic and gradient properties. In Chiappa, S. and Calandra, R. (eds.), *Proceedings of the Twenty Third International Conference on Artificial Intelligence and Statistics*, volume 108 of *Proceedings of Machine Learning Research*, pp. 2131–2141. PMLR, 26–28 Aug 2020.
- Flam-Shepherd, D., Requeima, J., and Duvenaud, D. Mapping Gaussian Process Priors to Bayesian Neural Networks. In *NeurIPS workshop on Bayesian Deep Learning*, 2017.
- Foret, P., Kleiner, A., Mobahi, H., and Neyshabur, B. Sharpness-Aware Minimization for Efficiently Improving Generalization. In *International Conference on Learning Representations*, 2021.
- Gal, Y. and Ghahramani, Z. Dropout As a Bayesian Approximation: Representing Model Uncertainty in Deep Learning. In *Proceedings of the 33rd International Conference on International Conference on Machine Learning - Volume 48, ICML’16*, pp. 1050–1059. JMLR.org, 2016.
- Gneiting, T. and Raftery, A. E. Strictly Proper Scoring Rules, Prediction, and Estimation. *Journal of the American Statistical Association*, 102:359–378, 2007.
- Goodfellow, I., Pouget-Abadie, J., Mirza, M., Xu, B., Warde-Farley, D., Ozair, S., Courville, A., and Bengio, Y. Generative Adversarial Nets. In Ghahramani, Z., Welling, M., Cortes, C., Lawrence, N., and Weinberger, K. (eds.), *Advances in Neural Information Processing Systems*, volume 27. Curran Associates, Inc., 2014.
- Gretton, A., Borgwardt, K., Rasch, M., Schölkopf, B., and Smola, A. A Kernel Method for the Two-Sample-Problem. In Schölkopf, B., Platt, J., and Hoffman, T. (eds.), *Advances in Neural Information Processing Systems*, volume 19. MIT Press, 2006.
- Gretton, A., Borgwardt, K. M., Rasch, M. J., Schölkopf, B., and Smola, A. A Kernel Two-Sample Test. *Journal of Machine Learning Research*, 13(25):723–773, 2012.

- Gulrajani, I., Ahmed, F., Arjovsky, M., Dumoulin, V., and Courville, A. C. Improved Training of Wasserstein GANs. In Guyon, I., Luxburg, U. V., Bengio, S., Wallach, H., Fergus, R., Vishwanathan, S., and Garnett, R. (eds.), *Advances in Neural Information Processing Systems*, volume 30. Curran Associates, Inc., 2017.
- Hochreiter, S. and Schmidhuber, J. Flat Minima. *Neural Computation*, 9(1):1–42, 01 1997. ISSN 0899-7667. doi: 10.1162/neco.1997.9.1.1.
- Huang, Y., Gokaslan, A., Kuleshov, V., and Tompkin, J. The GAN is dead; long live the GAN! A Modern GAN Baseline. In Globerson, A., Mackey, L., Belgrave, D., Fan, A., Paquet, U., Tomczak, J., and Zhang, C. (eds.), *Advances in Neural Information Processing Systems*, volume 37, pp. 44177–44215. Curran Associates, Inc., 2024.
- Jolicoeur-Martineau, A. The relativistic discriminator: a key element missing from standard GAN. In *International Conference on Learning Representations*, 2019.
- Karras, T., Laine, S., and Aila, T. A Style-Based Generator Architecture for Generative Adversarial Networks. *CoRR*, abs/1812.04948, 2018.
- Karras, T., Aittala, M., Hellsten, J., Laine, S., Lehtinen, J., and Aila, T. Training Generative Adversarial Networks with Limited Data. In Larochelle, H., Ranzato, M., Hadsell, R., Balcan, M., and Lin, H. (eds.), *Advances in Neural Information Processing Systems*, volume 33, pp. 12104–12114. Curran Associates, Inc., 2020a.
- Karras, T., Laine, S., Aittala, M., Hellsten, J., Lehtinen, J., and Aila, T. Analyzing and Improving the Image Quality of StyleGAN. In *2020 IEEE/CVF Conference on Computer Vision and Pattern Recognition (CVPR)*, pp. 8107–8116, Los Alamitos, CA, USA, June 2020b. IEEE Computer Society. doi: 10.1109/CVPR42600.2020.00813.
- Karras, T., Aittala, M., Laine, S., Härkönen, E., Hellsten, J., Lehtinen, J., and Aila, T. Alias-Free Generative Adversarial Networks. In Ranzato, M., Beygelzimer, A., Dauphin, Y., Liang, P., and Vaughan, J. W. (eds.), *Advances in Neural Information Processing Systems*, volume 34, pp. 852–863. Curran Associates, Inc., 2021.
- Leshno, M., Lin, V. Y., Pinkus, A., and Schocken, S. Multilayer feedforward networks with a nonpolynomial activation function can approximate any function. *Neural Networks*, 6(6):861–867, 1993. ISSN 0893-6080. doi: [https://doi.org/10.1016/S0893-6080\(05\)80131-5](https://doi.org/10.1016/S0893-6080(05)80131-5).
- Li, C.-L., Chang, W.-C., Cheng, Y., Yang, Y., and Póczos, B. MMD GAN: Towards Deeper Understanding of Moment Matching Network. In Guyon, I., Luxburg, U. V., Bengio, S., Wallach, H., Fergus, R., Vishwanathan, S., and Garnett, R. (eds.), *Advances in Neural Information Processing Systems*, volume 30. Curran Associates, Inc., 2017.
- Li, Y., Swersky, K., and Zemel, R. Generative Moment Matching Networks. In Bach, F. and Blei, D. (eds.), *Proceedings of the 32nd International Conference on Machine Learning*, volume 37 of *Proceedings of Machine Learning Research*, pp. 1718–1727, Lille, France, 07–09 Jul 2015. PMLR.
- Liu, H., Simonyan, K., and Yang, Y. DARTS: Differentiable Architecture Search. In *International Conference on Learning Representations*, 2019.
- Loaiza-Ganem, G., Ross, B. L., Cresswell, J. C., and Caterini, A. L. Diagnosing and Fixing Manifold Overfitting in Deep Generative Models. *Transactions on Machine Learning Research*, 2022. ISSN 2835-8856.
- Mackay, D. J. C. Bayesian Methods for Backpropagation Networks. In Domany, E., van Hemmen, J. L., and Schulten, K. (eds.), *Models of Neural Networks III*, chapter 6, pp. 211–254. Springer, 1994.
- MacKay, D. J. C. Bayesian neural networks and density networks. *Nuclear Instruments and Methods in Physics Research A*, 354(1):73–80, February 1995. doi: 10.1016/0168-9002(94)00931-7.
- Mescheder, L., Nowozin, S., and Geiger, A. Adversarial Variational Bayes: Unifying Variational Autoencoders and Generative Adversarial Networks. In Precup, D. and Teh, Y. W. (eds.), *Proceedings of the 34th International Conference on Machine Learning*, volume 70 of *Proceedings of Machine Learning Research*, pp. 2391–2400. PMLR, 06–11 Aug 2017.
- Müller, A. Integral Probability Metrics and Their Generating Classes of Functions. *Advances in Applied Probability*, 29(2):429–443, 1997. doi: 10.2307/1428011.
- Nagarajan, V. and Kolter, J. Z. Gradient descent GAN optimization is locally stable. In Guyon, I., Luxburg, U. V., Bengio, S., Wallach, H., Fergus, R., Vishwanathan, S., and Garnett, R. (eds.), *Advances in Neural Information Processing Systems*, volume 30. Curran Associates, Inc., 2017.
- Neal, R. M. *Bayesian Learning for Neural Networks (Lecture Notes in Statistics)*. Springer, 1 edition, August 1996. ISBN 0387947248.
- Nguyen, X., Wainwright, M. J., and Jordan, M. Estimating divergence functionals and the likelihood ratio by penalized convex risk minimization. In Platt, J., Koller,

- D., Singer, Y., and Roweis, S. (eds.), *Advances in Neural Information Processing Systems*, volume 20. Curran Associates, Inc., 2007.
- Nie, W. and Patel, A. B. Towards a Better Understanding and Regularization of GAN Training Dynamics. In Adams, R. P. and Gogate, V. (eds.), *Proceedings of The 35th Uncertainty in Artificial Intelligence Conference*, volume 115 of *Proceedings of Machine Learning Research*, pp. 281–291. PMLR, 22–25 Jul 2020.
- Nowozin, S., Cseke, B., and Tomioka, R. f-GAN: Training Generative Neural Samplers using Variational Divergence Minimization. In Lee, D., Sugiyama, M., Luxburg, U., Guyon, I., and Garnett, R. (eds.), *Advances in Neural Information Processing Systems*, volume 29. Curran Associates, Inc., 2016.
- Radford, A., Metz, L., and Chintala, S. Unsupervised Representation Learning with Deep Convolutional Generative Adversarial Networks. In *4th International Conference on Learning Representations*, 2016.
- Roth, K., Lucchi, A., Nowozin, S., and Hofmann, T. Stabilizing Training of Generative Adversarial Networks through Regularization. In Guyon, I., Luxburg, U. V., Bengio, S., Wallach, H., Fergus, R., Vishwanathan, S., and Garnett, R. (eds.), *Advances in Neural Information Processing Systems*, volume 30. Curran Associates, Inc., 2017.
- Saatci, Y. and Wilson, A. G. Bayesian GAN. In Guyon, I., Luxburg, U. V., Bengio, S., Wallach, H., Fergus, R., Vishwanathan, S., and Garnett, R. (eds.), *Advances in Neural Information Processing Systems*, volume 30. Curran Associates, Inc., 2017.
- Schmidhuber, J. Making the world differentiable: on using self supervised fully recurrent neural networks for dynamic reinforcement learning and planning in non-stationary environments. *Forschungsberichte, TU Munich*, FKI 126 90:1–26, 1990.
- Schmidhuber, J. A Possibility for Implementing Curiosity and Boredom in Model-Building Neural Controllers. In *Proceedings of the First International Conference on Simulation of Adaptive Behavior on From Animals to Animals*, pp. 222–227, Cambridge, MA, USA, 1991. MIT Press. ISBN 0262631385.
- Schmidhuber, J. Discovering Solutions with Low Kolmogorov Complexity and High Generalization Capability. In *Proceedings of the Twelfth International Conference on International Conference on Machine Learning*, ICML’95, pp. 488–496, San Francisco, CA, USA, 1995. Morgan Kaufmann Publishers Inc. ISBN 1558603778.
- Sharma, M., Farquhar, S., Nalisnick, E., and Rainforth, T. Do Bayesian Neural Networks Need To Be Fully Stochastic? In Ruiz, F., Dy, J., and van de Meent, J.-W. (eds.), *Proceedings of The 26th International Conference on Artificial Intelligence and Statistics*, volume 206 of *Proceedings of Machine Learning Research*, pp. 7694–7722. PMLR, 25–27 Apr 2023.
- Sinha, S., Zhao, Z., Goyal, A., Raffel, C. A., and Odena, A. Top-k Training of GANs: Improving GAN Performance by Throwing Away Bad Samples. In Larochelle, H., Ranzato, M., Hadsell, R., Balcan, M., and Lin, H. (eds.), *Advances in Neural Information Processing Systems*, volume 33, pp. 14638–14649. Curran Associates, Inc., 2020.
- Solomonoff, R. A formal theory of inductive inference. Part I. *Information and Control*, 7(1):1–22, 1964. ISSN 0019-9958. doi: [https://doi.org/10.1016/S0019-9958\(64\)90223-2](https://doi.org/10.1016/S0019-9958(64)90223-2).
- Tiao, L. C., Bonilla, E. V., and Ramos, F. Cycle-Consistent Adversarial Learning as Approximate Bayesian Inference. *CoRR*, abs/1806.01771, 2018.
- Tran, B.-H., Rossi, S., Milios, D., Michiardi, P., Bonilla, E. V., and Filippone, M. Model Selection for Bayesian Autoencoders. In Ranzato, M., Beygelzimer, A., Dauphin, Y., Liang, P., and Vaughan, J. W. (eds.), *Advances in Neural Information Processing Systems*, volume 34, pp. 19730–19742. Curran Associates, Inc., 2021.
- Tran, B.-H., Rossi, S., Milios, D., and Filippone, M. All You Need is a Good Functional Prior for Bayesian Deep Learning. *Journal of Machine Learning Research*, 23 (74):1–56, 2022.
- Villani, C. *Optimal Transport: Old and New*. Grundlehren der mathematischen Wissenschaften. Springer Berlin Heidelberg, 2016. ISBN 9783662501801.
- Wang, Y., Wu, J., Hovakimyan, N., and Sun, R. Balanced Training for Sparse GANs. In *Proceedings of the 37th International Conference on Neural Information Processing Systems*, NIPS ’23, Red Hook, NY, USA, 2023a. Curran Associates Inc.
- Wang, Z., Zheng, H., He, P., Chen, W., and Zhou, M. Diffusion-GAN: Training GANs with Diffusion. In *International Conference on Learning Representations*, 2023b.
- Wu, J., Huang, Z., Thoma, J., Acharya, D., and Van Gool, L. Wasserstein Divergence for GANs. In *Computer Vision – ECCV 2018: 15th European Conference, Munich, Germany, September 8–14, 2018, Proceedings*,

*Part V*, pp. 673–688, Berlin, Heidelberg, 2018. Springer-Verlag. ISBN 978-3-030-01227-4. doi: 10.1007/978-3-030-01228-1\_40.

Zheng, H., Nie, W., Vahdat, A., Azizzadenesheli, K., and Anandkumar, A. Fast Sampling of Diffusion Models via Operator Learning. In Krause, A., Brunskill, E., Cho, K., Engelhardt, B., Sabato, S., and Scarlett, J. (eds.), *Proceedings of the 40th International Conference on Machine Learning*, volume 202 of *Proceedings of Machine Learning Research*, pp. 42390–42402. PMLR, 23–29 Jul 2023.

Zhu, J.-Y., Park, T., Isola, P., and Efros, A. A. Unpaired Image-to-Image Translation Using Cycle-Consistent Adversarial Networks. In *2017 IEEE International Conference on Computer Vision (ICCV)*, pp. 2242–2251, 2017. doi: 10.1109/ICCV.2017.244.

## A. Experiments using a larger batch size

In this section, we report results using a larger batch size. The results show poorer performance, but again the best configurations are associated with some form of regularization possibly in combination with SAM. Despite the effectiveness of SAM, even for a larger batch-size compared with the experiments in the main paper, flatter minima are generally not associated with better performance.

Table 2. Experiments using a larger batch-size  $|B| = 512$ .

			MNIST				CIFAR-10			
			W-GAN $ B  = 512$							
$\sigma_{\text{lik}}^2$	$\lambda_{\text{gr}}$	$\rho_{\text{SAM}}$	ISC $\uparrow$	FID $\downarrow$	KID $\times 10^{-3} \downarrow$	$\ell_1$	ISC $\uparrow$	FID $\downarrow$	KID $\times 10^{-3} \downarrow$	$\ell_1$
0.0	0.0	0.0	2.18 (0.02)	17.7 (0.9)	14.6 (1.0)	23.6 (10.2)	3.66 (0.16)	107.1 (3.9)	97.5 (4.1)	10.2 (6.8)
0.01	0.0	0.0	2.11 (0.12)	21.2 (5.3)	18.4 (6.1)	24.2 (12.4)	3.55 (0.08)	107.6 (5.8)	97.5 (6.3)	8.1 (3.2)
0.001	0.0	0.0	2.17 (0.02)	17.9 (1.0)	14.8 (1.0)	22.1 (12.2)	3.65 (0.13)	107.7 (3.6)	97.3 (3.6)	9.9 (7.4)
0.0	0.01	0.0	2.17 (0.02)	18.2 (0.9)	14.9 (0.9)	25.3 (10.9)	3.68 (0.07)	104.9 (4.6)	95.5 (5.6)	11.3 (5.6)
0.01	0.01	0.0	2.20 (0.02)	18.9 (0.3)	15.5 (0.2)	24.0 (9.5)	3.65 (0.11)	105.9 (5.8)	95.5 (5.8)	11.8 (9.9)
0.001	0.01	0.0	2.18 (0.03)	18.0 (0.5)	14.9 (0.5)	22.5 (7.8)	3.68 (0.16)	107.8 (4.7)	97.2 (4.8)	9.7 (7.8)
0.0	0.001	0.0	2.18 (0.02)	18.4 (0.5)	15.2 (0.6)	30.7 (8.3)	3.55 (0.13)	108.2 (4.4)	98.3 (4.8)	16.2 (3.4)
0.01	0.001	0.0	2.15 (0.08)	18.5 (1.3)	15.4 (1.6)	22.4 (9.2)	3.65 (0.18)	104.0 (3.7)	93.1 (4.4)	16.6 (6.2)
0.001	0.001	0.0	2.19 (0.01)	18.1 (1.0)	14.9 (1.0)	22.9 (9.4)	3.67 (0.09)	108.1 (2.6)	97.4 (2.6)	13.2 (4.7)
0.0	0.0	0.01	2.17 (0.02)	18.0 (0.5)	14.8 (0.5)	24.7 (9.5)	3.65 (0.10)	110.6 (6.8)	100.6 (7.6)	18.6 (8.4)
0.01	0.0	0.01	2.18 (0.02)	18.3 (0.7)	15.0 (0.6)	18.6 (4.9)	3.62 (0.06)	108.7 (4.2)	98.6 (3.6)	9.6 (2.8)
0.001	0.0	0.01	2.17 (0.02)	17.9 (0.7)	14.8 (0.5)	24.1 (3.2)	3.71 (0.13)	107.3 (2.8)	97.1 (4.4)	13.7 (2.7)
0.0	0.01	0.01	2.19 (0.02)	18.7 (0.7)	15.4 (0.8)	22.5 (7.7)	3.63 (0.07)	107.8 (3.0)	96.5 (3.1)	20.3 (11.4)
0.01	0.01	0.01	2.18 (0.03)	18.0 (0.4)	14.8 (0.4)	23.0 (9.6)	3.69 (0.17)	106.8 (6.9)	95.7 (7.6)	11.2 (10.2)
0.001	0.01	0.01	2.18 (0.02)	18.2 (0.8)	15.0 (0.8)	25.5 (12.8)	3.65 (0.08)	106.5 (6.0)	96.3 (6.6)	12.5 (5.8)
0.0	0.001	0.01	2.16 (0.03)	17.9 (0.8)	14.8 (1.0)	21.0 (9.7)	3.72 (0.08)	110.4 (6.6)	100.1 (6.7)	15.4 (12.0)
0.01	0.001	0.01	2.17 (0.02)	19.0 (2.2)	15.7 (2.3)	16.9 (8.6)	3.52 (0.13)	110.1 (4.3)	100.3 (4.6)	12.3 (6.0)
0.001	0.001	0.01	2.17 (0.02)	18.3 (0.7)	15.1 (0.7)	23.3 (6.1)	3.62 (0.11)	111.9 (8.8)	101.6 (9.3)	18.8 (12.4)
0.0	0.0	0.1	2.18 (0.01)	17.6 (0.5)	14.6 (0.5)	13.6 (2.4)	3.64 (0.10)	111.2 (4.9)	101.3 (4.9)	16.8 (5.1)
0.01	0.0	0.1	2.17 (0.02)	18.1 (0.8)	15.0 (0.8)	23.5 (8.5)	3.69 (0.14)	109.1 (8.2)	99.7 (8.9)	15.8 (6.3)
0.001	0.0	0.1	2.19 (0.03)	17.8 (0.4)	14.6 (0.4)	16.3 (11.5)	3.64 (0.10)	113.4 (6.8)	103.9 (8.3)	14.6 (7.8)
0.0	0.01	0.1	2.17 (0.01)	17.3 (0.6)	14.4 (0.6)	21.7 (9.9)	3.69 (0.09)	111.9 (5.8)	102.6 (6.2)	11.0 (5.6)
0.01	0.01	0.1	2.18 (0.01)	17.7 (1.0)	14.6 (0.8)	21.2 (12.1)	3.64 (0.11)	111.2 (5.0)	100.8 (5.6)	19.2 (8.0)
0.001	0.01	0.1	2.19 (0.02)	17.5 (0.6)	14.2 (0.6)	23.2 (4.0)	3.65 (0.12)	112.2 (5.9)	103.2 (6.4)	9.6 (5.3)
0.0	0.001	0.1	2.18 (0.02)	17.4 (0.7)	14.3 (0.8)	15.3 (4.9)	3.64 (0.23)	110.9 (3.7)	101.1 (4.5)	17.9 (6.6)
0.01	0.001	0.1	2.18 (0.02)	17.5 (0.9)	14.3 (0.8)	19.4 (8.7)	3.67 (0.13)	110.9 (3.9)	99.9 (4.2)	13.8 (6.5)
0.001	0.001	0.1	2.17 (0.02)	17.6 (0.5)	14.5 (0.5)	19.9 (8.2)	3.68 (0.14)	110.2 (2.5)	100.2 (3.5)	21.6 (7.4)

## B. Experiments using MCD with multiple Monte Carlo samples

In the experiments in the main paper, at each training iteration, we considered MCD with one Monte Carlo sample. A natural question is what happens when increasing the number of Monte Carlo samples, and as expected performance is generally improved.

Table 3. Comparison of MCD with one or five Monte Carlo samples during training.

			$N_{\text{MCD}} = 5$				$N_{\text{MCD}} = 1$			
			W-GAN $ B  = 128$				MNIST			
$\sigma_{\text{lik}}^2$	$\lambda_{\text{gr}}$	$\rho_{\text{SAM}}$	ISC $\uparrow$	FID $\downarrow$	KID $\times 10^{-3} \downarrow$	$\ell_1$	ISC $\uparrow$	FID $\downarrow$	KID $\times 10^{-3} \downarrow$	$\ell_1$
0.0	0.0	0.0	2.23 (0.00)	7.9 (0.1)	5.4 (0.1)	43.9 (0.0)	2.25 (0.02)	7.7 (0.5)	5.4 (0.5)	20.2 (15.1)
0.01	0.0	0.0	2.26 (0.01)	7.6 (0.0)	5.1 (0.0)	44.7 (0.0)	2.26 (0.02)	7.8 (0.3)	5.4 (0.3)	30.5 (11.8)
0.001	0.0	0.0	2.24 (0.01)	7.1 (0.0)	4.8 (0.1)	39.2 (0.0)	2.24 (0.01)	8.0 (0.3)	5.6 (0.4)	34.1 (8.3)
0.0	0.01	0.0	2.23 (0.02)	7.8 (0.1)	5.5 (0.2)	31.1 (0.0)	2.25 (0.01)	8.1 (0.8)	5.7 (0.8)	19.7 (8.7)
0.01	0.01	0.0	2.24 (0.01)	8.0 (0.2)	5.7 (0.3)	47.3 (0.0)	2.26 (0.02)	7.8 (0.3)	5.4 (0.3)	28.3 (11.4)
0.001	0.01	0.0	2.23 (0.00)	7.1 (0.1)	4.7 (0.0)	43.0 (0.0)	2.25 (0.02)	7.8 (0.2)	5.5 (0.3)	31.6 (10.0)
0.0	0.001	0.0	2.26 (0.02)	7.3 (0.1)	5.0 (0.1)	45.0 (0.0)	2.24 (0.01)	7.7 (0.4)	5.5 (0.4)	31.7 (10.9)
0.01	0.001	0.0	2.26 (0.01)	7.4 (0.1)	5.1 (0.1)	34.0 (0.0)	2.24 (0.01)	8.1 (0.4)	5.8 (0.4)	33.3 (7.2)
0.001	0.001	0.0	2.22 (0.01)	7.4 (0.1)	5.1 (0.2)	34.4 (0.0)	2.25 (0.01)	8.0 (0.7)	5.7 (0.7)	32.5 (8.4)

### C. Full set of results on W-GANs

In this section we report all results obtained by combining regularization strategies, SAM, and MCD on W-GANs. Even for this model, we found that regularization and SAM optimization generally lead to better performance.

Table 4. DC-GAN architecture with Wasserstein divergence objective (Wu et al., 2018) on MNIST and CIFAR-10. Standard deviations, calculated over five seeds times three repetitions of sampling 10 000 images, are reported in parenthesis.

			MNIST				CIFAR-10			
			W-GAN $ B  = 128$				W-GAN $ B  = 128$			
$\sigma_{\text{lik}}^2$	$\lambda_{\text{gr}}$	$\rho_{\text{SAM}}$	ISC $\uparrow$	FID $\downarrow$	KID $\times 10^{-3} \downarrow$	$\ell_1$	ISC $\uparrow$	FID $\downarrow$	KID $\times 10^{-3} \downarrow$	$\ell_1$
0.0	0.0	0.0	2.27 (0.02)	8.4 (0.4)	6.0 (0.4)	61.6 (8.3)	4.64 (0.13)	40.1 (1.5)	30.3 (1.6)	11.6 (5.9)
0.01	0.0	0.0	2.27 (0.02)	8.0 (0.4)	5.5 (0.4)	55.5 (15.1)	4.74 (0.08)	34.1 (2.2)	24.1 (2.1)	11.2 (3.6)
0.001	0.0	0.0	2.27 (0.02)	8.3 (0.3)	5.9 (0.3)	68.8 (13.5)	4.72 (0.11)	37.2 (2.8)	27.4 (2.6)	6.6 (3.8)
0.0	0.01	0.0	2.26 (0.01)	8.2 (0.4)	5.8 (0.4)	59.4 (15.4)	4.72 (0.08)	37.8 (1.3)	27.9 (1.6)	4.6 (3.3)
0.01	0.01	0.0	2.26 (0.01)	8.3 (0.3)	5.9 (0.3)	67.0 (11.1)	4.79 (0.11)	34.2 (1.7)	24.2 (1.9)	12.3 (4.2)
0.001	0.01	0.0	2.25 (0.01)	8.3 (0.3)	6.0 (0.3)	61.5 (10.7)	4.71 (0.07)	37.4 (1.9)	27.6 (2.1)	9.8 (4.0)
0.0	0.001	0.0	2.27 (0.02)	8.0 (0.2)	5.5 (0.2)	61.7 (14.3)	4.68 (0.14)	40.3 (3.3)	30.7 (3.4)	10.2 (5.1)
0.01	0.001	0.0	2.27 (0.02)	8.4 (0.5)	6.0 (0.4)	58.4 (11.8)	4.76 (0.11)	33.8 (3.8)	23.7 (4.1)	9.1 (5.4)
0.001	0.001	0.0	2.26 (0.01)	8.1 (0.4)	5.7 (0.4)	8.6 (22.3)	4.76 (0.11)	40.0 (1.9)	30.3 (2.1)	13.4 (4.9)
0.0	0.0	0.01	2.25 (0.01)	8.4 (0.2)	6.0 (0.2)	62.4 (5.4)	4.70 (0.09)	39.2 (2.2)	29.4 (2.4)	8.7 (6.5)
0.01	0.0	0.01	2.27 (0.02)	8.0 (0.2)	5.5 (0.3)	58.0 (3.2)	4.74 (0.08)	36.7 (2.2)	26.5 (2.2)	10.4 (2.0)
0.001	0.0	0.01	2.26 (0.02)	8.0 (0.2)	5.6 (0.3)	57.5 (16.1)	4.70 (0.11)	41.7 (3.8)	32.3 (4.1)	15.6 (2.6)
0.0	0.01	0.01	2.27 (0.02)	8.1 (0.3)	5.7 (0.4)	69.9 (16.8)	4.79 (0.10)	39.6 (2.8)	30.1 (2.9)	9.5 (3.1)
0.01	0.01	0.01	2.27 (0.02)	8.3 (0.5)	5.8 (0.5)	72.8 (22.6)	4.79 (0.10)	33.8 (2.4)	23.5 (2.3)	9.7 (3.6)
0.001	0.01	0.01	2.26 (0.01)	8.5 (0.5)	6.1 (0.5)	65.2 (11.6)	4.74 (0.10)	39.7 (2.8)	29.9 (2.6)	6.7 (4.1)
0.0	0.001	0.01	2.27 (0.02)	8.1 (0.4)	5.7 (0.4)	64.2 (12.1)	4.76 (0.08)	38.7 (2.9)	28.9 (3.1)	9.9 (4.2)
0.01	0.001	0.01	2.26 (0.01)	8.2 (0.3)	5.8 (0.3)	63.6 (6.3)	4.78 (0.07)	33.2 (1.1)	23.1 (1.3)	9.6 (2.0)
0.001	0.001	0.01	2.26 (0.02)	8.3 (0.3)	5.9 (0.3)	58.4 (8.5)	4.65 (0.16)	41.9 (5.1)	32.1 (5.2)	7.9 (2.7)
0.0	0.0	0.1	2.25 (0.02)	8.6 (0.4)	6.2 (0.5)	54.7 (5.9)	4.68 (0.15)	40.6 (3.4)	31.2 (3.5)	11.7 (2.1)
0.01	0.0	0.1	2.26 (0.02)	8.5 (0.5)	6.0 (0.5)	43.4 (4.6)	4.76 (0.07)	37.2 (2.1)	27.5 (2.3)	7.5 (3.0)
0.001	0.0	0.1	2.26 (0.02)	8.4 (0.3)	6.0 (0.3)	48.0 (14.4)	4.71 (0.09)	40.9 (2.8)	31.7 (3.3)	10.9 (3.3)
0.0	0.01	0.1	2.26 (0.02)	8.0 (0.4)	5.5 (0.3)	53.1 (8.5)	4.74 (0.11)	40.4 (2.0)	31.2 (2.0)	7.7 (3.7)
0.01	0.01	0.1	2.27 (0.02)	8.1 (0.4)	5.7 (0.4)	49.1 (3.7)	4.76 (0.13)	36.0 (2.3)	26.0 (2.3)	6.4 (6.4)
0.001	0.01	0.1	2.24 (0.02)	8.1 (0.3)	5.7 (0.3)	49.8 (3.7)	4.76 (0.09)	40.7 (4.1)	31.8 (4.4)	10.9 (1.2)
0.0	0.001	0.1	2.25 (0.02)	8.3 (0.5)	6.0 (0.5)	45.2 (6.4)	4.75 (0.05)	39.5 (3.4)	30.5 (3.7)	9.6 (4.1)
0.01	0.001	0.1	2.26 (0.01)	8.2 (0.3)	5.8 (0.3)	58.2 (15.5)	4.81 (0.11)	37.2 (4.3)	27.5 (4.5)	10.4 (3.4)
0.001	0.001	0.1	2.25 (0.01)	8.3 (0.3)	6.0 (0.3)	43.8 (8.5)	4.80 (0.13)	38.8 (3.6)	29.5 (3.7)	11.6 (4.2)
			W-GAN $ B  = 128$				WITH MCD			
0.0	0.0	0.0	2.25 (0.02)	7.7 (0.5)	5.4 (0.5)	20.2 (15.1)	4.75 (0.05)	38.6 (2.2)	28.7 (2.2)	18.7 (6.2)
0.01	0.0	0.0	2.26 (0.02)	7.8 (0.3)	5.4 (0.3)	30.5 (11.8)	4.87 (0.20)	32.8 (2.9)	22.1 (2.8)	13.6 (8.0)
0.001	0.0	0.0	2.24 (0.01)	8.0 (0.3)	5.6 (0.4)	34.1 (8.3)	4.79 (0.08)	40.2 (3.2)	29.5 (3.2)	14.1 (6.3)
0.0	0.01	0.0	2.25 (0.01)	8.1 (0.8)	5.7 (0.8)	19.7 (8.7)	4.72 (0.07)	39.8 (3.7)	29.2 (3.9)	19.0 (8.1)
0.01	0.01	0.0	2.26 (0.02)	7.8 (0.3)	5.4 (0.3)	28.3 (11.4)	4.77 (0.15)	35.9 (2.6)	25.1 (2.5)	23.8 (12.6)
0.001	0.01	0.0	2.25 (0.02)	7.8 (0.2)	5.5 (0.3)	31.6 (10.0)	4.73 (0.08)	38.7 (1.9)	28.2 (1.8)	10.4 (6.4)
0.0	0.001	0.0	2.24 (0.01)	7.7 (0.4)	5.5 (0.4)	31.7 (10.9)	4.80 (0.09)	37.7 (3.3)	27.0 (3.3)	15.2 (10.7)
0.01	0.001	0.0	2.24 (0.01)	8.1 (0.4)	5.8 (0.4)	33.3 (7.2)	4.73 (0.08)	33.9 (2.7)	23.3 (3.0)	9.7 (4.2)
0.001	0.001	0.0	2.25 (0.01)	8.0 (0.7)	5.7 (0.7)	32.5 (8.4)	4.66 (0.15)	40.6 (1.9)	29.9 (2.2)	22.7 (10.7)
0.0	0.0	0.01	2.25 (0.02)	7.8 (0.4)	5.4 (0.4)	35.6 (5.7)	4.75 (0.12)	38.0 (3.6)	27.2 (3.3)	16.1 (5.3)
0.01	0.0	0.01	2.26 (0.02)	7.9 (0.2)	5.5 (0.2)	27.8 (15.7)	4.81 (0.07)	34.5 (2.8)	23.7 (3.1)	17.9 (11.2)
0.001	0.0	0.01	2.25 (0.02)	7.8 (0.5)	5.5 (0.6)	24.3 (9.9)	4.80 (0.08)	39.2 (4.4)	28.8 (4.1)	18.6 (6.9)
0.0	0.01	0.01	2.25 (0.02)	7.6 (0.4)	5.2 (0.4)	32.8 (7.7)	4.77 (0.15)	39.3 (3.1)	28.6 (2.7)	15.8 (3.2)
0.01	0.01	0.01	2.25 (0.01)	7.6 (0.3)	5.3 (0.2)	24.3 (7.3)	4.82 (0.09)	33.2 (1.4)	22.4 (1.4)	24.0 (8.8)
0.001	0.01	0.01	2.25 (0.02)	8.0 (0.4)	5.8 (0.3)	30.0 (5.7)	4.69 (0.06)	37.3 (2.2)	26.8 (2.3)	14.3 (5.1)
0.0	0.001	0.01	2.25 (0.02)	7.8 (0.3)	5.4 (0.3)	31.0 (12.6)	4.67 (0.09)	38.8 (3.7)	28.4 (3.8)	20.0 (5.1)
0.01	0.001	0.01	2.23 (0.02)	7.8 (0.4)	5.5 (0.4)	25.3 (4.8)	4.84 (0.17)	34.4 (1.8)	23.6 (1.8)	19.4 (9.2)
0.001	0.001	0.01	2.25 (0.01)	8.1 (0.3)	5.7 (0.3)	26.3 (6.4)	4.80 (0.05)	38.3 (2.9)	27.8 (3.2)	14.0 (2.2)
0.0	0.0	0.1	2.25 (0.01)	7.6 (0.4)	5.2 (0.4)	24.2 (4.2)	4.86 (0.08)	38.9 (3.3)	28.4 (3.5)	14.4 (3.7)
0.01	0.0	0.1	2.25 (0.02)	7.7 (0.3)	5.2 (0.3)	28.0 (11.9)	4.76 (0.10)	35.3 (3.3)	24.9 (3.4)	12.4 (6.8)
0.001	0.0	0.1	2.25 (0.01)	7.8 (0.3)	5.4 (0.2)	17.4 (4.2)	4.74 (0.07)	40.6 (2.2)	30.1 (2.1)	12.4 (5.3)
0.0	0.01	0.1	2.25 (0.02)	7.7 (0.2)	5.3 (0.2)	26.0 (2.2)	4.78 (0.11)	39.0 (3.9)	28.6 (3.8)	16.1 (8.4)
0.01	0.01	0.1	2.25 (0.02)	7.2 (0.1)	4.8 (0.2)	20.2 (7.5)	4.76 (0.06)	36.0 (2.5)	25.3 (2.6)	11.8 (4.9)
0.001	0.01	0.1	2.25 (0.01)	7.8 (0.3)	5.4 (0.3)	29.8 (4.9)	4.71 (0.10)	41.8 (2.6)	31.3 (2.6)	14.2 (7.7)
0.0	0.001	0.1	2.24 (0.01)	7.5 (0.3)	5.1 (0.3)	21.6 (14.4)	4.77 (0.12)	38.9 (2.3)	28.4 (2.4)	14.4 (4.0)
0.01	0.001	0.1	2.25 (0.02)	7.9 (0.3)	5.5 (0.3)	21.8 (11.5)	4.72 (0.07)	37.9 (2.8)	27.0 (2.6)	7.0 (3.7)
0.001	0.001	0.1	2.25 (0.02)	7.7 (0.3)	5.4 (0.3)	28.7 (6.8)	4.72 (0.07)	40.6 (5.4)	30.7 (5.5)	13.4 (3.5)

Bridging GANs and Bayesian Neural Networks via Partial Stochasticity

Table 5. DC-GAN architecture with Wasserstein divergence objective (Wu et al., 2018) on FFHQ-128 and CELEBA. Standard deviations, calculated over five seeds times three repetitions of sampling 10 000 images, are reported in parenthesis.

			FFHQ-128				CELEBA			
			W-GAN $ B  = 128$							
$\sigma_{\text{lik}}^2$	$\lambda_{\text{gr}}$	$\rho_{\text{SAM}}$	ISC $\uparrow$	FID $\downarrow$	KID $\times 10^{-3} \downarrow$	$\ell_1$	ISC $\uparrow$	FID $\downarrow$	KID $\times 10^{-3} \downarrow$	$\ell_1$
0.0	0.0	0.0	3.21 (0.05)	63.6 (1.5)	55.8 (1.5)	45.9 (13.7)	2.87 (0.04)	18.3 (0.9)	12.4 (1.1)	31.2 (9.9)
0.01	0.0	0.0	3.25 (0.04)	62.8 (1.5)	54.8 (1.6)	51.6 (19.4)	2.89 (0.05)	17.8 (2.6)	11.5 (2.7)	26.4 (11.7)
0.001	0.0	0.0	3.24 (0.03)	63.2 (0.9)	55.6 (0.7)	49.7 (13.5)	2.87 (0.03)	18.4 (0.6)	12.4 (0.6)	25.6 (13.3)
0.0	0.01	0.0	3.22 (0.04)	65.1 (3.5)	57.0 (3.4)	37.9 (9.4)	2.88 (0.03)	18.5 (0.9)	12.6 (1.1)	33.4 (8.8)
0.01	0.01	0.0	3.24 (0.03)	63.5 (2.6)	55.7 (2.8)	48.5 (20.9)	2.87 (0.08)	24.8 (16.9)	18.6 (16.6)	30.0 (15.8)
0.001	0.01	0.0	3.20 (0.04)	66.3 (3.0)	58.3 (2.8)	43.2 (17.2)	2.88 (0.03)	18.1 (0.8)	12.0 (0.9)	22.9 (11.5)
0.0	0.001	0.0	3.24 (0.05)	62.9 (1.9)	54.9 (1.9)	43.4 (14.6)	2.88 (0.02)	17.9 (0.8)	11.9 (0.8)	18.0 (11.0)
0.01	0.001	0.0	3.26 (0.07)	62.1 (3.0)	54.2 (3.5)	33.8 (10.2)	2.90 (0.03)	25.4 (19.1)	19.0 (18.4)	35.9 (13.3)
0.001	0.001	0.0	3.22 (0.04)	64.9 (2.2)	57.5 (2.7)	31.5 (24.9)	2.88 (0.03)	17.2 (0.8)	11.1 (0.9)	32.4 (12.0)
0.0	0.0	0.01	3.22 (0.04)	62.9 (3.5)	55.4 (4.0)	38.2 (14.3)	2.89 (0.05)	28.2 (18.0)	21.7 (17.2)	20.2 (10.5)
0.01	0.0	0.01	3.25 (0.03)	61.6 (1.4)	53.8 (1.5)	46.0 (12.5)	2.90 (0.05)	18.4 (3.7)	12.2 (3.4)	26.6 (14.4)
0.001	0.0	0.01	3.21 (0.04)	64.6 (4.7)	56.7 (4.9)	29.9 (17.1)	2.88 (0.03)	17.8 (0.7)	12.1 (0.6)	39.9 (5.5)
0.0	0.01	0.01	3.22 (0.06)	63.1 (3.9)	55.2 (4.0)	54.6 (16.8)	2.91 (0.02)	18.4 (1.1)	12.5 (1.2)	32.8 (8.2)
0.01	0.01	0.01	3.26 (0.03)	61.2 (2.5)	53.0 (2.6)	40.1 (16.9)	2.90 (0.03)	15.9 (0.5)	10.0 (0.6)	38.0 (13.2)
0.001	0.01	0.01	3.22 (0.03)	62.4 (3.1)	54.4 (3.5)	31.2 (19.9)	2.90 (0.05)	17.4 (0.9)	11.5 (1.0)	31.3 (14.1)
0.0	0.001	0.01	3.24 (0.03)	61.8 (2.6)	53.8 (2.8)	43.9 (8.5)	2.91 (0.04)	17.7 (0.6)	11.7 (0.7)	29.5 (11.6)
0.01	0.001	0.01	3.24 (0.03)	64.3 (2.1)	56.7 (2.4)	33.7 (18.7)	2.91 (0.03)	16.4 (1.0)	10.5 (1.2)	43.6 (10.4)
0.001	0.001	0.01	3.23 (0.03)	62.5 (1.5)	54.8 (1.8)	50.9 (17.9)	2.89 (0.02)	18.2 (1.0)	12.3 (1.0)	33.2 (11.6)
0.0	0.0	0.1	3.26 (0.05)	62.1 (2.0)	53.9 (2.3)	37.1 (10.9)	2.84 (0.09)	34.9 (20.8)	28.5 (20.1)	19.3 (17.4)
0.01	0.0	0.1	3.27 (0.03)	60.8 (2.7)	52.8 (2.8)	47.2 (9.4)	2.86 (0.12)	29.7 (16.7)	23.3 (16.0)	18.3 (11.4)
0.001	0.0	0.1	3.25 (0.04)	60.9 (2.3)	53.1 (2.9)	43.4 (12.5)	2.85 (0.09)	25.8 (16.1)	20.1 (15.4)	26.1 (7.0)
0.0	0.01	0.1	3.22 (0.04)	62.1 (2.4)	54.2 (2.5)	30.6 (17.0)	2.90 (0.08)	37.6 (24.0)	32.6 (25.0)	18.6 (6.3)
0.01	0.01	0.1	3.27 (0.04)	58.5 (1.0)	50.1 (1.4)	40.4 (13.8)	2.86 (0.09)	29.0 (17.3)	22.1 (16.0)	28.5 (18.6)
0.001	0.01	0.1	3.21 (0.05)	63.0 (2.5)	55.2 (2.7)	47.6 (14.5)	2.85 (0.07)	35.3 (20.8)	29.7 (20.5)	25.6 (14.2)
0.0	0.001	0.1	3.20 (0.04)	62.9 (4.7)	55.2 (4.6)	40.0 (11.1)	2.87 (0.08)	24.6 (13.2)	18.6 (12.2)	27.9 (17.8)
0.01	0.001	0.1	3.26 (0.03)	60.2 (1.9)	51.8 (2.1)	34.4 (8.7)	2.87 (0.13)	29.5 (16.8)	23.4 (16.7)	21.1 (16.2)
0.001	0.001	0.1	3.25 (0.05)	63.2 (2.5)	55.0 (2.5)	38.8 (10.6)	2.87 (0.06)	31.4 (16.0)	24.8 (14.7)	10.0 (3.2)
			W-GAN $ B  = 128$ WITH				MCD			
0.0	0.0	0.0	3.20 (0.06)	65.5 (3.6)	57.4 (3.6)	36.1 (19.0)	2.95 (0.13)	42.9 (19.4)	34.9 (18.2)	24.1 (8.8)
0.01	0.0	0.0	3.24 (0.04)	67.5 (3.0)	59.1 (2.5)	46.3 (8.3)	2.83 (0.12)	60.8 (22.0)	55.3 (22.6)	19.5 (9.0)
0.001	0.0	0.0	3.19 (0.04)	63.1 (3.4)	55.1 (3.9)	48.4 (14.0)	3.01 (0.11)	65.0 (23.1)	58.3 (22.8)	20.0 (17.1)
0.0	0.01	0.0	3.17 (0.04)	67.4 (3.7)	59.3 (3.4)	49.7 (19.1)	3.02 (0.11)	81.1 (8.1)	75.7 (11.2)	25.1 (17.7)
0.01	0.01	0.0	3.25 (0.05)	62.8 (1.5)	55.1 (2.0)	44.2 (15.4)	2.83 (0.14)	70.4 (8.8)	64.1 (9.9)	29.0 (29.6)
0.001	0.01	0.0	3.20 (0.06)	65.0 (1.8)	56.9 (1.5)	40.3 (18.2)	2.95 (0.17)	76.1 (2.7)	70.3 (4.9)	33.4 (11.6)
0.0	0.001	0.0	3.19 (0.03)	66.7 (3.0)	58.4 (3.6)	20.3 (16.7)	2.96 (0.08)	59.8 (27.6)	53.8 (28.8)	31.0 (11.3)
0.01	0.001	0.0	3.23 (0.04)	64.6 (3.5)	56.8 (3.4)	48.0 (7.8)	2.93 (0.08)	63.5 (24.5)	57.4 (25.8)	19.7 (9.0)
0.001	0.001	0.0	3.21 (0.04)	64.3 (2.1)	56.1 (2.3)	27.0 (11.3)	3.11 (0.06)	76.9 (6.1)	67.8 (7.1)	28.7 (6.8)
0.0	0.0	0.01	3.19 (0.05)	68.9 (2.5)	60.8 (2.7)	46.1 (13.3)	2.98 (0.11)	68.3 (25.6)	63.0 (26.4)	27.8 (5.3)
0.01	0.0	0.01	3.22 (0.06)	66.6 (2.7)	58.1 (3.2)	35.6 (21.2)	2.94 (0.07)	66.0 (11.5)	57.1 (15.3)	32.5 (22.4)
0.001	0.0	0.01	3.20 (0.04)	67.7 (1.6)	59.7 (1.8)	57.6 (11.4)	2.88 (0.07)	41.7 (24.5)	34.8 (24.6)	14.6 (8.0)
0.0	0.01	0.01	3.19 (0.07)	65.3 (4.2)	57.2 (4.4)	38.3 (13.1)	2.92 (0.15)	75.3 (14.6)	71.0 (17.3)	29.5 (17.3)
0.01	0.01	0.01	3.21 (0.05)	65.3 (3.7)	57.5 (3.8)	59.8 (27.0)	2.84 (0.06)	44.8 (25.5)	37.9 (26.1)	20.3 (16.4)
0.001	0.01	0.01	3.19 (0.04)	63.3 (2.0)	55.0 (1.9)	77.7 (28.9)	2.88 (0.06)	81.8 (8.4)	80.1 (10.9)	14.0 (5.3)
0.0	0.001	0.01	3.18 (0.03)	63.2 (3.0)	55.2 (3.4)	61.2 (29.4)	2.81 (0.12)	69.7 (5.2)	64.2 (6.2)	20.7 (5.2)
0.01	0.001	0.01	3.23 (0.06)	67.2 (4.8)	59.0 (4.5)	46.6 (22.0)	2.89 (0.06)	52.5 (29.1)	47.4 (30.2)	23.5 (9.1)
0.001	0.001	0.01	3.21 (0.09)	66.8 (5.0)	58.3 (5.3)	86.0 (95.1)	2.80 (0.14)	59.9 (21.7)	54.2 (21.5)	26.3 (10.0)
0.0	0.0	0.1	3.19 (0.04)	66.5 (4.1)	58.1 (4.2)	42.0 (19.0)	2.89 (0.08)	40.1 (27.0)	34.2 (27.5)	29.2 (6.9)
0.01	0.0	0.1	3.23 (0.04)	62.8 (3.1)	54.7 (3.5)	50.8 (16.4)	2.83 (0.11)	51.5 (29.3)	47.7 (31.6)	14.7 (8.0)
0.001	0.0	0.1	3.18 (0.04)	64.5 (1.8)	56.1 (1.8)	38.3 (26.5)	2.98 (0.12)	60.1 (23.7)	52.7 (24.0)	17.4 (10.9)
0.0	0.01	0.1	3.21 (0.05)	63.7 (4.8)	55.3 (5.1)	27.7 (18.1)	2.81 (0.10)	49.8 (25.7)	45.2 (26.7)	24.1 (15.3)
0.01	0.01	0.1	3.23 (0.04)	62.6 (4.0)	54.7 (4.2)	46.2 (24.3)	2.95 (0.06)	67.0 (25.9)	60.8 (26.5)	24.1 (15.0)
0.001	0.01	0.1	3.20 (0.03)	61.7 (1.2)	52.7 (1.0)	43.1 (23.3)	2.87 (0.13)	68.2 (16.7)	63.8 (19.6)	12.6 (6.8)
0.0	0.001	0.1	3.21 (0.06)	61.7 (2.2)	53.1 (2.3)	55.3 (20.8)	2.85 (0.13)	49.4 (27.8)	43.4 (28.7)	28.8 (24.9)
0.01	0.001	0.1	3.23 (0.04)	61.4 (2.6)	53.0 (2.9)	36.0 (19.2)	2.84 (0.09)	50.0 (27.1)	43.3 (26.9)	17.8 (16.9)
0.001	0.001	0.1	3.19 (0.06)	65.6 (5.4)	56.7 (5.5)	61.4 (20.4)	2.94 (0.18)	74.5 (7.8)	69.0 (10.8)	13.1 (6.5)

### D. Results on R-GANs

In this section, we report results on R-GANs, which we generally found to be more unstable to train compared to W-GANs.

Table 6. DC-GAN architecture with the objective of R-GANs (Jolicoeur-Martineau, 2019) on MNIST, CIFAR-10, FFHQ-128, and CELEBA. Standard deviations, calculated over five seeds times three repetitions of sampling 10 000 images, are reported in parenthesis. The arrows indicate whether metrics are so that the higher the better ( $\uparrow$ ) or the lower the better ( $\downarrow$ ).  $|B|$  denotes the batch size.

R-GAN $ B  = 128$								
STRATEGY	MNIST				CIFAR-10			
	ISC $\uparrow$	FID $\downarrow$	KID $\times 10^{-3}$ $\downarrow$	$\ell_1$	ISC $\uparrow$	FID $\downarrow$	KID $\times 10^{-3}$ $\downarrow$	$\ell_1$
NONE	1.93 (0.46)	101.8 (184.3)	134.7 (257.7)	1165.7 (1313.3)	5.01 (0.12)	21.0 (1.7)	10.8 (1.5)	63.4 (30.8)
LIKELIHOOD RELAX. ( $\sigma_{\text{lik}}^2 = 0.01$ )	1.79 (0.67)	251.8 (172.3)	306.2 (272.1)	1582.6 (838.7)	2.40 (0.40)	239.3 (33.0)	168.7 (37.9)	6692.6 (6632.2)
GRADIENT REG. ( $\lambda_{\text{gr}} = 0.01$ )	1.92 (0.46)	111.5 (141.1)	119.9 (191.0)	2774.3 (2475.6)	5.16 (0.10)	19.6 (1.4)	9.4 (0.8)	61.1 (34.2)
SAM ( $\rho_{\text{SAM}} = 0.1$ )	2.14 (0.02)	9.2 (0.9)	5.7 (0.8)	2802.8 (3767.8)	5.19 (0.13)	19.7 (0.7)	9.9 (0.5)	65.0 (42.1)
MCD ( $p = 0.1$ )	2.11 (0.11)	50.3 (49.6)	41.9 (46.4)	1330.1 (1174.8)	4.92 (0.05)	21.6 (0.2)	11.8 (0.3)	918.8 (588.8)

FFHQ-128								
STRATEGY	FFHQ-128				CELEBA			
	ISC $\uparrow$	FID $\downarrow$	KID $\times 10^{-3}$ $\downarrow$	$\ell_1$	ISC $\uparrow$	FID $\downarrow$	KID $\times 10^{-3}$ $\downarrow$	$\ell_1$
NONE	3.38 (0.05)	54.2 (4.8)	42.9 (4.5)	65.8 (50.7)	2.82 (0.10)	22.6 (2.2)	9.7 (0.8)	37.3 (19.8)
LIKELIHOOD RELAX. ( $\sigma_{\text{lik}}^2 = 0.01$ )	3.08 (0.25)	91.2 (24.0)	73.6 (18.8)	154.8 (203.3)	1.32 (0.32)	399.3 (44.8)	471.0 (79.9)	3909.8 (4234.7)
GRADIENT REG. ( $\lambda_{\text{gr}} = 0.01$ )	3.34 (0.10)	56.2 (5.2)	45.3 (6.6)	34.7 (28.2)	2.79 (0.08)	23.0 (2.2)	9.5 (1.4)	66.7 (47.6)
SAM ( $\rho_{\text{SAM}} = 0.1$ )	3.33 (0.10)	52.7 (3.0)	41.1 (4.3)	50.3 (17.2)	2.77 (0.03)	24.3 (2.6)	10.4 (2.0)	37.6 (38.0)
MCD ( $p = 0.1$ )	3.34 (0.11)	53.0 (2.7)	44.7 (2.8)	80.4 (86.7)	2.76 (0.03)	20.1 (1.8)	11.1 (1.9)	59.9 (49.9)